Journal of Science and Technology in Civil Engineering NUCE 2019. 13 (2): 48–63

# WEIGHT OPTIMISATION OF FUNCTIONALLY GRADED BEAMS USING MODIFIED DIFFERENTIAL EVOLUTION

Pham Hoang Anh[a,*], Tran Thuy Duong[a]

[a]*Faculty of Building and Industrial Construction, National University of Civil Engineering, 55 Giai Phong road, Hai Ba Trung district, Hanoi, Vietnam*

***Article history:***
*Received 07/12/2018, Revised 08/03/2019, Accepted 23/04/2019*

**Abstract**

In this article, an efficient numerical approach for weight optimisation of functionally graded (FG) beams in the presence of frequency constraints is presented. For the analysis purpose, a finite element (FE) solution based on the first order shear deformation theory (FSDT) is established to analyse the free vibration behaviour of FG beams. A four-parameter power law distribution and a five-parameter trigonometric distribution are used to describe the volume fraction of material constituents in the thickness direction. The goal is to tailor the thickness and material distribution for minimising the weight of FG beams while constraining the fundamental frequency to be greater than a prescribed value. The constrained optimisation problem is effectively solved by a novel differential evolution (DE) algorithm. The validity and efficiency of the proposed approach is demonstrated through two numerical examples corresponding to the four-parameter distribution and the five-parameter distribution.

*Keywords:* FGM beam; lightweight design; frequency constraint; differential evolution.

https://doi.org/10.31814/stce.nuce2019-13(2)-05 

## 1. Introduction

In recent decades the development of a new kind of materials, functionally graded materials (FGMs), has opened great opportunities for optimal structural design. FGMs are advanced materials composed of two or more constituents that have continuous and smooth spatial variation of the relative volume fraction and microstructure [1]. With advantageous characteristics such as high temperature resistant and elimination of stress concentration, FGMs are increasingly and widely used in different fields such as aerospace, marine, mechanical and structural engineering. In an FGM, material composition can be tailored to derive maximum benefits from its inhomogeneity [2]. Thus, optimisation of material distribution for structures made of FGMs has drawn considerable research attention.

On the other hand, frequency constraints are essential in structural design to improve the performance of a structure and to prevent the resonance phenomenon [3]. The optimal structural design under frequency constraints is a well-known optimisation problem, whereas the weight or an objective function value corresponding to the minimal cost of a structure is minimised while satisfying frequency constraints. There have been numerous researches on the optimal design of FG beams in the dynamic regime (e.g. [2, 4–10]). However, most of the published works considered the optimal

*Corresponding author. *E-mail address:* anhpham.nuce@gmail.com (Anh, P. H.)

design for maximising/minimising the fundamental frequency. Studies have rarely been conducted on the lightweight design of FG beams. Therefore, the aim of the present study is to optimise the thickness and material distribution to minimising the weight of FG beams in the presence of frequency constraints.

The considered optimisation problem is highly nonlinear and difficult to solve by conventional gradient-based techniques. Metaheuristics (MHs), which do not rely on the function derivative and are suitable for nonlinear, non-convex, multimodal optimisation problems, have become dominant in the optimisation of FG beams. Some well-established MHs have been applied, including the genetic algorithm (GA) [2, 4, 9], differential evolution (DE) [7, 8, 10], and the firefly algorithm [6]. To effectively solve the optimisation problem of FG beams, a new optimisation algorithm based on differential evolution, termed modified differential evolution with directional mutation and nearest neighbour comparison (DErdn), is introduced in this article. DE is a simple population-based, stochastic optimiser which has shown good global search ability for various optimisation problems. However, like many population-based MHs, one of the main issues in applying DE is its expensive computation requirement. The proposed enhancements in the present work attempt to reduce the computation burden and enhance the search ability of DE. These enhancements are relatively simple and do not introduce additional control parameters as often appeared in other modified DE variants.

The determination of the natural frequencies requires the solution of the free vibration problem. There have been many published works on the analysis of the free vibration of FG beams using analytical approaches (e.g. see [11–15]). In this study, to accommodate different boundary conditions, the finite element (FE) method is utilised. The formulation of the FG beam element is based on the first order shear deformation theory (FSDT) and linear elastic analysis. It is noted that FSDT has been used to develop the finite element solution for the vibration analysis of FG beams by Chakraborty et al. [16] using the simple power law for the volume fraction. Here, this finite element formulation is extended for FG beams with a four-parameter power law distribution and a five-parameter trigonometric distribution of the volume fraction in beam's thickness direction. These distribution formulations are supposed to permit more diverse material distributions for optimisation purpose. The four-parameter and five-parameter distributions have been used by some researchers for material distribution through the longitudinal direction to maximise the fundamental frequency of FG beams [9] and arches [10].

## 2. Free vibration of FG beam

Consider an FG beam composed of two materials with the length $L$ and rectangular cross section $b \times h$, where $b$ is the width and $h$ is the height (Fig. 1). The $x$, $y$ and $z$-coordinates are taken along the length, width and height of the beam, respectively.

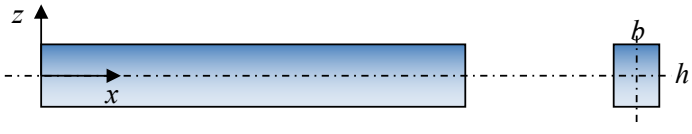


Figure 1. Functionally graded beam

### 2.1. Formula for volume fraction

The material properties are assumed to vary continuously along the thickness of the beam (in the $z$-direction) and governed by the volume fraction of its constituents according to the linear rule of

mixtures:

$$P(z) = P_1 V_1(z) + P_2 V_2(z); \quad V_2(z) = 1 - V_1(z) \tag{1}$$

where $P$ represents the effective material property such as Young's modulus $E$, and mass density $\rho$; $V$ is the volume fraction; subscripts 1 and 2 represent the constituent 1 and constituent 2, respectively. Possible distribution laws for volume fraction are the power law [17], the sigmoid law [18], the exponential law [19] and the three-parameter law [20]. In this study, to spatially tailor the material properties, it is proposed that the volume fraction of constituent 1 follows a four-parameter power law distribution or a five-parameter trigonometric distribution as given in Table 1.

Table 1. Volume fraction of constituent 1

| Four-parameter power law distribution | Five-parameter trigonometric distribution |
|---|---|
| $V_1 = a\left[\frac{1}{2} + \frac{z}{h} + b\left(\frac{1}{2} - \frac{z}{h}\right)^c\right]^p$ | $V_1 = a\left[\frac{1}{2} - \frac{b}{2}\sin\left(c\pi\left(\frac{1}{2} - \frac{z}{h}\right) + d\right)\right]^p$ |

The parameters $a$, $b$, $c$, $d$, and $p$ are the model parameters and are treated as design variables. The proposed formulas are supposed to allow diverse material distributions for optimisation purpose. It is noted that the four-parameter power law distribution can be transformed to the simple power law distribution of Eq. (2) by setting $a = 1$ and $b = 0$.

$$V_1 = \left[\frac{1}{2} + \frac{z}{h}\right]^p \tag{2}$$

### *2.2. FE solution for free vibration of FG beam*

a. Governing equations

Based on the first-order shear deformation theory (or the Timoshenko beam theory), the displacement field is given as

$$\begin{aligned} u(x, z, t) &= u_0(x, t) - z\phi(x, t) \\ w(x, z, t) &= w_0(x, t) \end{aligned} \tag{3}$$

where $u$ and $w$ are the displacements at a point along $x$ and $z$ directions; $u_0$ and $w_0$ are the axial and transverse displacement on the mid-surface, respectively; $\phi$ is the rotation of the cross section about the $y$-axis. Assuming linear elastic material behaviour, the strains are determined as:

$$\begin{aligned} \varepsilon_x &= \frac{\partial u}{\partial x} = \frac{\partial u_0}{\partial x} - z\frac{\partial \phi}{\partial x} \\ \gamma_{xz} &= \frac{\partial u}{\partial z} + \frac{\partial w}{\partial x} = \frac{\partial w_0}{\partial x} - \phi \end{aligned} \tag{4}$$

and stresses are of the form:

$$\begin{aligned} \sigma_x &= E(z)\varepsilon_x \\ \tau_{xz} &= \frac{E(z)}{2(1+\nu)}\gamma_{xz} = G(z)\gamma_{xz}; \quad G(z) = \frac{E(z)}{2(1+\nu)} \end{aligned} \tag{5}$$

where $\sigma_x$ and $\varepsilon_x$ are the normal stress and normal strain in the $x$ direction; $\tau_{xz}$ and $\gamma_{xz}$ are the shear stress and shear strain in the $x - z$ plane; $E(z)$ and $G(z)$ are the Young's modulus and shear modulus, with $E(z)$ is computed from the mixture rule of Eq. (1).

Applying the principle of virtual work to the free vibration problem of the beam leads to:

$$b\int_0^L\int_{-h/2}^{h/2}(\sigma_x\delta\varepsilon_x+\tau_{xz}\delta\gamma_{xz})dzdx+b\int_0^L\int_{-h/2}^{h/2}\rho(z)\left(\frac{\partial^2u}{\partial t^2}\delta u+\frac{\partial^2w}{\partial t^2}\delta w\right)dzdx=0 \tag{6}$$

where the symbol $\delta$ denotes the variation operator. By substituting Eqs. (4) and (5) into Eq. (6), integrating by parts and noting that the variation $\delta u_0$, $\delta w_0$ and $\delta\phi$ can be arbitrary, we obtain the following governing equations:

$$\begin{aligned}
&-A_{11}\frac{\partial^2u_0}{\partial x^2}+B_{11}\frac{\partial^2\phi}{\partial x^2}+I_0\frac{\partial^2u_0}{\partial t^2}-I_1\frac{\partial^2\phi}{\partial t^2}=0\\
&-A_{55}\left(\frac{\partial^2w_0}{\partial x^2}-\frac{\partial\phi}{\partial x}\right)+I_0\frac{\partial^2w_0}{\partial t^2}=0\\
&-B_{11}\frac{\partial^2u_0}{\partial x^2}+D_{11}\frac{\partial^2\phi}{\partial x^2}+A_{55}\left(\frac{\partial w_0}{\partial x}-\phi\right)+I_1\frac{\partial^2u_0}{\partial t^2}-I_2\frac{\partial^2\phi}{\partial t^2}=0
\end{aligned} \tag{7}$$

where the coefficients $A_{11}$, $B_{11}$, $D_{11}$, $A_{55}$, $I_0$, $I_1$, and $I_2$ are given by:

$$\begin{aligned}
(A_{11},B_{11},D_{11})&=b\int_{-h/2}^{h/2}E(z)(1,z,z^2)dz\\
A_{55}&=kb\int_{-h/2}^{h/2}G(z)dz\\
(I_0,I_1,I_2)&=b\int_{-h/2}^{h/2}\rho(z)(1,z,z^2)dz
\end{aligned} \tag{8}$$

The stress resultants are

$$\begin{aligned}
N_x&=b\int_{-h/2}^{h/2}\sigma_xdz=A_{11}\frac{\partial u_0}{\partial x}-B_{11}\frac{\partial\phi}{\partial x}\\
Q_x&=kb\int_{-h/2}^{h/2}\gamma_{xz}dz=A_{55}\left(\frac{\partial w_0}{\partial x}-\phi\right)\\
M_x&=b\int_{-h/2}^{h/2}-z\sigma_xdz=-B_{11}\frac{\partial u_0}{\partial x}+D_{11}\frac{\partial\phi}{\partial x}
\end{aligned} \tag{9}$$

In Eqs. (8) and (9), $k$ is the shear correction factor ($k = 5/6$), which is required to compensate for the error due to the assumption in FSDT.

b. Finite element formulation

According to Ref. [16], the interpolation functions for the displacement field of a finite beam element have the form:

$$\begin{aligned} u_0 &= c_1 + c_2 x + c_3 x^2 \\ w_0 &= c_4 + c_5 x + c_6 x^2 + c_7 x^3 \\ \phi &= c_8 + c_9 x + c_{10} x^2 \end{aligned} \tag{10}$$

Substituting Eqs. (10) into the static part of the governing equations given by Eq. (7), the following relations can be derived

$$c_3 = c_{10}\frac{B_{11}}{A_{11}}, \quad c_7 = \frac{c_{10}}{3}, \quad c_6 = \frac{c_9}{2}, \quad c_{10} = \frac{A_{11}A_{55}}{2(A_{11}D_{11} - B_{11}^2)}(c_8 - c_5) \tag{11}$$

The interpolation functions are then rewritten as

$$\begin{aligned} u_0 &= c_1 + c_2 x + \frac{1}{2}\alpha(c_8 - c_5)x^2 \\ w_0 &= c_4 + c_5 x + \frac{c_9}{2}x^2 + \frac{1}{6}\beta(c_8 - c_5)x^3 \\ \phi &= c_8 + c_9 x + \frac{1}{2}\beta(c_8 - c_5)x^2 \end{aligned} \tag{12}$$

where $\alpha = \dfrac{B_{11}A_{55}}{(A_{11}D_{11} - B_{11}^2)}, \beta = \dfrac{A_{11}A_{55}}{(A_{11}D_{11} - B_{11}^2)}$, or in matrix form

$$\{u\} = \{u_0, w_0, \phi\}^T = [N(x)]\{c\},$$

$$\{c\} = \begin{Bmatrix} c_1 \\ c_2 \\ c_4 \\ c_5 \\ c_8 \\ c_9 \end{Bmatrix}, \quad [N(x)] = \begin{bmatrix} 1 & x & 0 & -\dfrac{x^2\alpha}{2} & \dfrac{x^2\alpha}{2} & 0 \\ 0 & 0 & 1 & x - \dfrac{x^3\beta}{6} & \dfrac{x^3\beta}{6} & \dfrac{x^2}{2} \\ 0 & 0 & 0 & -\dfrac{x^2\beta}{2} & 1 + \dfrac{x^2\beta}{2} & x \end{bmatrix} \tag{13}$$

The vector of independent constants $\{c\}$ can be expressed in terms of nodal displacements by using boundary conditions for each node, (at $x = 0$ and $x = L$):

$$\begin{Bmatrix} u(0) \\ u(L) \end{Bmatrix} = \begin{bmatrix} N(0) \\ N(L) \end{bmatrix}\{c\}, \quad \{c\} = \begin{bmatrix} N(0) \\ N(L) \end{bmatrix}^{-1}\begin{Bmatrix} u(0) \\ u(L) \end{Bmatrix} = [G]\{\hat{u}\} \tag{14}$$

where $\{\hat{u}\} = \{u_1, w_1, \phi_1, u_2, w_2, \phi_2\}^T$ is the vector of nodal displacements of the element.

The displacements of a point in the element can be expressed in terms of nodal displacements:

$$\{u\} = [N(x)][G]\{\hat{u}\} = [\aleph(x)]\{\hat{u}\} \tag{15}$$

where the matrix $[\aleph(x)] = [\aleph_u(x) \quad \aleph_w(x) \quad \aleph_\phi(x)]^T$, with $\aleph_u(x)$, $\aleph_w(x)$ and $\aleph_\phi(x)$ being the exact shape functions for axial, transverse and rotational degrees of freedom, respectively [16]. The expression for the shape functions are given in Appendix A.

Now, the force resultants in Eq. (9) can be written in terms of the nodal displacements:

$$\begin{aligned} N_x &= \left(A_{11}\frac{\partial \aleph_u}{\partial x} - B_{11}\frac{\partial \aleph_\phi}{\partial x}\right)\{\hat{u}\} \\ Q_x &= A_{55}\left(\frac{\partial \aleph_w}{\partial x} - \aleph_\phi\right)\{\hat{u}\} \\ M_x &= \left(-B_{11}\frac{\partial \aleph_u}{\partial x} + D_{11}\frac{\partial \aleph_\phi}{\partial x}\right)\{\hat{u}\} \end{aligned} \tag{16}$$

Using Eq. (16), we can derive the element force vector as:

$$\{F\} = \{-N_x(0), -Q_x(0), -M_x(0), N_x(L), Q_x(L), M_x(L)\}^T = [K]\{\hat{u}\} \tag{17}$$

where $[K]$ is the element stiffness matrix, and its explicit form is given in Appendix B.

The consistent element mass matrix is expressed as summation of four sub-matrices [16]

$$[M] = [M_u] + [M_w] + [M_\phi] + [M_{u\phi}] \tag{18}$$

where the components of the consistent mass matrix are determined as follows

$$\begin{aligned} [M_u] &= \int_0^L I_0[\aleph_u]^T[\aleph_u]dx \\ [M_w] &= \int_0^L I_0[\aleph_w]^T[\aleph_w]dx \\ [M_\phi] &= \int_0^L I_2[\aleph_\phi]^T[\aleph_\phi]dx \\ [M_{u\phi}] &= -\int_0^L I_1\left([\aleph_u]^T[\aleph_\phi] + [\aleph_\phi]^T[\aleph_u]\right)dx \end{aligned} \tag{19}$$

The system equations are obtained by assembly of element matrices, implementation of boundary conditions, and introduction of loads. The free vibration behaviour of the beam is obtained by solving the following eigenproblem

$$([\mathbf{K}] - \omega^2[\mathbf{M}])\{\mathbf{u}\} = \{0\} \tag{20}$$

where $[\mathbf{K}]$, $[\mathbf{M}]$ and $\{\mathbf{u}\}$ are the system stiffness matrix, system mass matrix and system nodal displacement vector; $\omega$ is the circular natural frequency of the beam. The eigenvalues are determined from the condition that the determinant of the system of equations given by Eq. (19) must vanish.

### *2.3. Verification of FE solution*

To verify the FE solution, an FG beam made of aluminium (Al; $E_m$ = 70 GPa, $\rho_m$ = 2702 kg/m$^3$, $\nu_m$ = 0.3) and alumina ($Al_2O_3$; $E_c$ = 380 GPa, $\rho_c$ = 3960 kg/m$^3$, $\nu_c$ = 0.3) taken from Ref. [12] is considered. The volume fraction of alumina follows the simple power-law given by Eq. (2). Beams

with various support condition (SC), including pinned-pinned (PP), clamped-clamped (CC), clamped-pinned (CP), and clamped-free (CF) are examined. For comparison purpose, the non-dimensional frequency [12], $\Omega = (\omega L^2 \sqrt{\rho_m/E_m})/h$, is utilised.

Table 2 shows the convergence of the non-dimensional fundamental frequency with various numbers of elements of the FG beam with $h = 0.1$ m, $L/h = 5$, and $p = 1$. It is seen from Table 2 that numerical accuracy of the frequencies is satisfactory when the number of elements is 50. Using 50

Table 2. Convergence study for FG beams with $L/h = 5$, and $p = 1$

| Number of elements | PP | CC | CP | CF |
|---|---|---|---|---|
| 10 | 3.9721 | 7.9096 | 5.8440 | 1.4628 |
| 20 | 3.9712 | 7.9022 | 5.8410 | 1.4628 |
| 30 | 3.9710 | 7.9008 | 5.8405 | 1.4628 |
| 40 | 3.9709 | 7.9004 | 5.8403 | 1.4628 |
| 50 | 3.9709 | 7.9001 | 5.8402 | 1.4628 |
| 100 | 3.9709 | 7.8998 | 5.8401 | 1.4628 |

equal elements, the non-dimensional frequencies are calculated and compared with those in Ref. [12] obtained by analytical solution using FSDT for $L/h = 5$ and 20 in Tables 3 and 4, respectively. As seen from Tables 3 and 4, the results from FE analysis (FEA) agree well with the results by Simsek [12] and the difference between the frequencies of the two studies is very small (less than one percent).

Table 3. Comparison of non-dimensional fundamental frequencies with $L/h = 5$

| SC | Method | $p$ | | | | | |
|---|---|---|---|---|---|---|---|
| | | 0 | 0.5 | 1 | 2 | 5 | 10 |
| PP | FSDT [12] | 5.15247 | 4.40830 | 3.99023 | 3.63438 | 3.43119 | 3.31343 |
| | FEA | 5.1526 | 4.3989 | 3.9709 | 3.6047 | 3.4023 | 3.2961 |
| CC | FSDT [12] | 10.0344 | 8.70047 | 7.92529 | 7.21134 | 6.66764 | 6.34062 |
| | FEA | 9.9981 | 8.6709 | 7.9001 | 7.1883 | 6.6432 | 6.3152 |
| CF | FSDT [12] | 1.89479 | 1.61737 | 1.46300 | 1.33376 | 1.26445 | 1.22398 |
| | FEA | 1.8944 | 1.6169 | 1.4628 | 1.3335 | 1.2642 | 1.2237 |

## 3. Optimisation problem

The optimisation problem considered in this study is the minimisation of the weight of an FG beam while keeping its fundamental frequency to be greater than a prescribed value. The material distribution and the thickness are optimised simultaneously. The problem is formulated as

$$\begin{aligned} &\text{Minimise } W(a,b,c,d,p,h) = \int_{-h/2}^{h/2} \rho(z)dz \\ &\text{Subject to } f_1 \geq f_{\min} \end{aligned} \tag{21}$$

Table 4. Comparison of non-dimensional fundamental frequencies with $L/h = 20$

| SC | Method | $p$ | | | | | |
|---|---|---|---|---|---|---|---|
| | | 0 | 0.5 | 1 | 2 | 5 | 10 |
| PP | FSDT [12] | 5.46032 | 4.65137 | 4.20505 | 3.83676 | 3.65088 | 3.54156 |
| | FEA | 5.4603 | 4.6503 | 4.2037 | 3.8347 | 3.6488 | 3.5403 |
| CC | FSDT [12] | 12.2235 | 10.4263 | 9.43135 | 8.60401 | 8.16985 | 7.91275 |
| | FEA | 12.2202 | 10.4229 | 9.4292 | 8.6021 | 8.1676 | 7.9102 |
| CF | FSDT [12] | 1.94957 | 1.66044 | 1.50104 | 1.36968 | 1.30375 | 1.26495 |
| | FEA | 1.9495 | 1.6603 | 1.5010 | 1.3697 | 1.3037 | 1.2649 |

where $W$ is the weight per unit length; $f_1$ is the fundamental frequency; and $f_{\min}$ is a frequency lower limit. In the above optimisation problem, the design variables $a$, $b$, $c$, $d$, $p$ and $h$ must be chosen such that the volume fraction at any point along the height will stay within the permissible physical limits, that is $0 \leq V_1 \leq 1$. To assure that, an additional set of constraints is introduced as:

$$\begin{aligned} 0 \leq V_{1,top}, V_{1,bottom} \leq 1 \\ 0 \leq V_{1,\min}; \quad V_{1,\max} \leq 1 \end{aligned} \tag{22}$$

where $V_{1,top}, V_{1,bottom}$ are the volume fraction values at the boundaries (at the top and the bottom); and $V_{1,\min}, V_{1,\max}$ are the minima and maxima within the structure domain. The maxima/minima point $z_{opt}$ can be obtained by solving:

$$V_1'(z) = 0 \tag{23}$$

For the four-parameter power law distribution, we obtained:

$$z_{opt} = \frac{h}{2}\left(1 - 2\mathrm{e}^{\frac{-\log[b]-\log[c]}{c-1}}\right) \tag{24}$$

For the five-parameter trigonometric distribution, we obtained:

$$z_{opt} = \begin{cases} \dfrac{h\,(2d - \pi + c\pi)}{2c\pi} \\ \dfrac{h\,(2d + \pi + c\pi)}{2c\pi} \\ \dfrac{h}{2c\pi}\left(2d + c\pi - 2\arcsin\left[\dfrac{1 - 20^{\frac{1}{-1+p}}}{b}\right]\right) \end{cases} \tag{25}$$

The values of the volume fraction at the points in the structure domain corresponding to these extrema should satisfy the permissible limits.

## 4. Modified differential evolution

In this section, a novel differential evolution algorithm, termed as DErdn, is presented for solving the above optimisation problem. The enhancement is established through two modifications to the conventional DE, which are: 1) The random directional mutation for increasing the possibility of creating improved solutions; and 2) the nearest neighbour comparison method to prejudge a solution so that unpromising solution will be skipped without evaluating it.

### *4.1. Basic differential evolution*

Differential evolution (DE) invented by Storn and Price [21] is a population-based optimiser. DE uses a population of $NP$ candidate vectors of the design variables $\mathbf{x}_k,\ k = 1, 2, ..., NP$, (individuals), and an individual is defined as $\mathbf{x}_k = (x_{k1}, x_{k2}, ..., x_{kD})$, where $x_{ki}, i = 1, 2, ..., D$, are the design variables and $D$ is the dimension of the optimisation problem. The population is then restructured by survival individuals evolutionally. First, an initial population is randomly sampled from the solution space as shown in Eq. (26):

$$x_{ki} = x_i^l + \text{rand}[0, 1] \times (x_i^u - x_i^l), \qquad i = 1, 2, ..., D \tag{26}$$

where $x_i^l$ and $x_i^u$ are the lower and upper bounds of the $i$-th design variable $x_i$, respectively, and rand[0, 1] is a uniformly distributed random real value in the range [0, 1].

Then, each individual $\mathbf{x}_k$ (called the target vector) of the current population is compared with a newly generated vector (called the trial vector) and the better one will be selected as a new member of the population of next generation. The evolution proceeds until a termination criterion is met.

Two operators, named as 'mutation' and 'crossover', are used for producing trial vectors and they are described as follows.

**Mutation**: For each target vector $\mathbf{x}_k$, a mutant vector $\mathbf{y}_k$ is first generated. Various mutation strategies can be employed to create the mutant vector. The most popular one in classical DE is the so-called 'DE/rand/1', where the mutant vector is determined as:

$$\mathbf{y}_k = \mathbf{x}_{r_1} + F \times (\mathbf{x}_{r_2} - \mathbf{x}_{r_3}) \tag{27}$$

where $\mathbf{x}_{r_1}, \mathbf{x}_{r_2}, \mathbf{x}_{r_3}$ are three mutually different individuals randomly selected from the current population, that is $r_1 \neq r_2 \neq r_3 \neq k$; $F$ is a scaling factor, a real and constant factor usually chosen in the interval [0, 1] which controls the amplification of the differential variation. In Eq. (26), $\mathbf{x}_{r_1}$ is called the base vector, while the others are called the difference vectors.

**Crossover**: Crossover is introduced to exchange the information of the mutant vector with the target vector $\mathbf{x}_k$, creating a trial vector $\mathbf{z}_k$ with its elements determined by:

$$z_{ki} = \begin{cases} y_{ki}, & \text{if (rand}[0, 1] \leq Cr) \text{ or } (r = i) \\ x_{ki}, & \text{otherwise} \end{cases} \tag{28}$$

where $r$ is a randomly chosen integer in the interval $[1, D]$ to ensure that the trial vector has at least one element from the mutant vector; $Cr$ is the crossover rate predefined in [0, 1], which control the fraction of elements copied from the mutant vector.

### *4.2. Modification in mutation: the random directional mutation*

In the mutation operator of Eq. (26), a random variation is derived from the difference of two randomly selected different individuals. Consequently, it has no bias to any special search directions. To take advantage of guiding information of the population, the differential variation is multiplied by a 'directed' factor $d$, which takes either value 1 or $-1$ depending on the order relation between the difference vectors $\mathbf{x}_{r_2}$ and $\mathbf{x}_{r_3}$,

$$d = \begin{cases} 1, & \text{if } \mathbf{x}_{r_2} \text{ is better than } \mathbf{x}_{r_3} \\ -1, & \text{otherwise} \end{cases} \tag{29}$$

This kind of directional mutation has the same concept of the well-known opposition based method presented for improving the DE performance in the literature [22, 23]. This rule guarantees that the differential variation is oriented toward a better vector, thus increasing the possibility of creating an improved solution.

Furthermore, random scaling factors are introduced to increase the diversity of the trial vector. The new mutation, named as 'random directional mutation', operator has the form

$$y_{ki} = x_{r_1 i} + d \times \text{rand}[0, 1] \times (x_{r_2 i} - x_{r_3 i}) \tag{30}$$

### *4.3. Modification in selection: the nearest neighbour comparison*

In conventional DE, function evaluations are required for all trial vectors and many of them do not survive in the selection phase. Thus, many evaluations are useless. It is desirable that trial vectors that might produce no better fitness should not be evaluated. It is particularly important in problems where function evaluation is costly. A method called 'Nearest neighbour comparison' (NNC) is a recently developed method by Pham [24], which can effectively reduce the number of function evaluations for various unconstraint benchmark optimisation problems. In this study, the NNC method is employed to reduce unnecessary function evaluations in solving constrained optimisation problem. The method is briefly described as follows.

Firstly, for each trial vector $\mathbf{z}_k$, a vector $\mathbf{z}_k^{nn}$ in the current population which is closest to $\mathbf{z}_k$ is sought using the normalised Euclidean distance measure:

$$d(\mathbf{x}, \mathbf{z}_k) = \sqrt{\sum_{i=1}^{D} \left( \frac{x_i - z_{ki}}{x_i^{\max} - x_i^{\min}} \right)^2} \tag{31}$$

where $d(\mathbf{x}, \mathbf{z}_k)$ is the distance measure between two vectors $\mathbf{x}$ and $\mathbf{z}_k$; $x_i^{\max}$ and $x_i^{\min}$ are the current maximum and minimum values of the corresponding design variable $x_i$ of all solutions in the population. Thus, $\mathbf{z}_k^{nn}$ is the vector in the current population with the smallest distance to the trial vector $\mathbf{z}_k$.

Secondly, $\mathbf{z}_k^{nn}$ is compared with the target vector $\mathbf{x}_k$. If $\mathbf{z}_k^{nn}$ is worse than $\mathbf{x}_k$, the trial vector is likely worse than the target vector and it will be skipped. Otherwise, the trial vector is evaluated for further selection decision. In this way, several unpromising trial vectors are omitted and useless function evaluations can be reduced during the searching process.

### *4.4. Handling of constraints and comparison of solutions*

The considered optimisation problem has inequality constraints, which can be expressed in the form

$$c_j(\mathbf{x}_k) \leq 0, \quad j = 1, 2, ..., N_C \tag{32}$$

where $N_C$ is the number of constraints of the optimisation problem and $c_j(\mathbf{x}_k)$ is the $j$-th constraint function. The constraint violation of a solution $\mathbf{x}_k$ is then determined as

$$C_k = \max \left\{ \max_j \{0, c_j(\mathbf{x}_k)\} \right\}, \quad j = 1, 2, ..., N_C \tag{33}$$

Deb's rules [25] are employed in this study to handle inequality constraints and to compare two solutions. Deb's constraint rules have been successfully applied to the GA and several MHs, and are described as:

1) A feasible solution is better than any infeasible one.

2) Of two feasible solutions or two solutions with equal constraint violations, the one having a smaller objective function value is the better one.

3) Of two infeasible solutions, the one having a smaller constraint violation is the better one.

## 5. Illustration examples

To demonstrate the efficiency of the proposed numerical approach, the lightweight design optimisation of an FG beam with length $L = 1$ is performed. The beam has the material properties similar as those given in Section 2.3. Two optimisation problems are considered. In the first problem (Problem 1), the volume fraction of alumina follows the four-parameter distribution. In the second problem (Problem 2), the five-parameter distribution is utilised. For both problems, the lower bound for the fundamental frequency of the beam is 500 Hz. The ranges of the design variables for each problem are given in Table 5. These ranges are chosen based on a preliminary investigation of the proposed models of volume fraction given in Table 1, which ensure a wide range of possibilities for material distribution.

Table 5. Design variable ranges

| Design variable | $a$ | $b$ | $c$ | $d$ | $p$ |
|---|---|---|---|---|---|
| Problem 1 | [0, 1] | [0, 20] | [0, 20] | NA | [0, 20] |
| Problem 2 | [0, 1] | [0, 1] | [-2, 2] | $[-\pi, \pi]$ | [0, 20] |

First, to better understand the performance of DErdn, the influence of each modification introduced in DErdn is investigated. Four different algorithms, including the conventional 'DE/rand/1' (DE), the DE with random scaling factor (DEr), the DE with random scaling factor and the directional mutation (DErd), and the DE with all proposed modifications, i.e. DErdn, are examined for this purpose. The parameter setting is as follows: the population size $NP = 50$; the maximum iteration $T_{\max} = 300$ for Problem 1 and 200 for Problem 2; the scaling factor $F = 0.8$ (applicable only for 'DE/rand/1'); the cross-over rate $Cr = 0.9$ for 'DE/rand/1' and 1 for the other algorithms. Each algorithm is run 20 times to obtain statistical results.

Tables 6 and 7 present the optimisation results for Problems 1 and 2 with pinned-pinned supports, respectively. The statistical results include the best solution, the best, mean, worst, standard deviation (SD) values of optimal weights and the average number of function evaluations (NFEs). It is seen that DEr, DErd and DErdn produce better results than DE does, while DErd gives the best results. It is obvious that the DErdn with the nearest neighbour operator reduces the number of function evaluations considerably.

Fig. 2 plots the average convergences of the best-found weight over the number of function evaluations for different algorithms. Clearly, all the modified DE algorithms converge faster than the classical DE does, and DErdn is the fastest algorithm. Fig. 2 also shows that the directional mutation does have considerable influence on the convergence rate.

Now, DErdn is used to optimise beams with different support conditions. The best optimal results in 20 random runs are presented for Problems 1 and 2 in Tables 8 and 9, respectively. As expected, the optimised beam with fixed ends has the lightest weight while the optimised cantilever beam has the largest weight, and all the optimised beams have the fundamental frequency satisfied the constraint.

Table 6. Optimisation results of Problem 1 obtained by different algorithms

| | DE | DEr | DErd | DErdn |
|---|---|---|---|---|
| $a$ | 0.9978 | 0.9999 | 1.0000 | 0.9996 |
| $b$ | 1.0000 | 1.0000 | 1.0000 | 1.0001 |
| $c$ | 2.4989 | 2.5246 | 2.4358 | 2.4692 |
| $p$ | 4.6675 | 4.5262 | 4.7531 | 4.7027 |
| $h$ [m] | 0.1295 | 0.1291 | 0.1292 | 0.1293 |
| Best $W$ [kg/m] | 410.1711 | 410.0551 | 410.0488 | 410.0498 |
| $f_1$ (Hz) | 500.0015 | 500.0002 | 500.0047 | 500.0010 |
| Mean $W$ [kg/m] | 417.5693 | 414.7205 | 410.0940 | 412.1080 |
| Worst $W$ [kg/m] | 434.9078 | 435.9859 | 410.3107 | 428.9328 |
| SD | 9.6828 | 8.5115 | 0.0658 | 5.6677 |
| NFEs | 15000 | 15000 | 15000 | 8065 |

Table 7. Optimisation results of Problem 2 obtained by different algorithms

| | DE | DEr | DErd | DErdn |
|---|---|---|---|---|
| $a$ | 0.9994 | 1.0000 | 1.0000 | 1.0000 |
| $b$ | 0.9998 | 1.0000 | 1.0000 | 1.0000 |
| $c$ | −1.9995 | −1.9998 | 2.0000 | −2.0000 |
| $d$ | −1.5733 | −1.5665 | −1.5705 | -1.5714 |
| $p$ | 2.1086 | 2.0444 | 2.0123 | 2.0439 |
| $h$ [m] | 0.1205 | 0.1202 | 0.1201 | 0.1202 |
| Best $W$ [kg/m] | 381.1445 | 381.0108 | 381.0033 | 381.0057 |
| $f_1$ (Hz) | 500.0709 | 500.0004 | 500.0012 | 500.0011 |
| Mean $W$ [kg/m] | 381.9820 | 381.0617 | 381.0137 | 381.0196 |
| Worst $W$ [kg/m] | 384.2704 | 381.2963 | 381.0365 | 381.0728 |
| SD | 0.7220 | 0.0632 | 0.00756 | 0.0158 |
| NFEs | 10000 | 10000 | 10000 | 5478 |

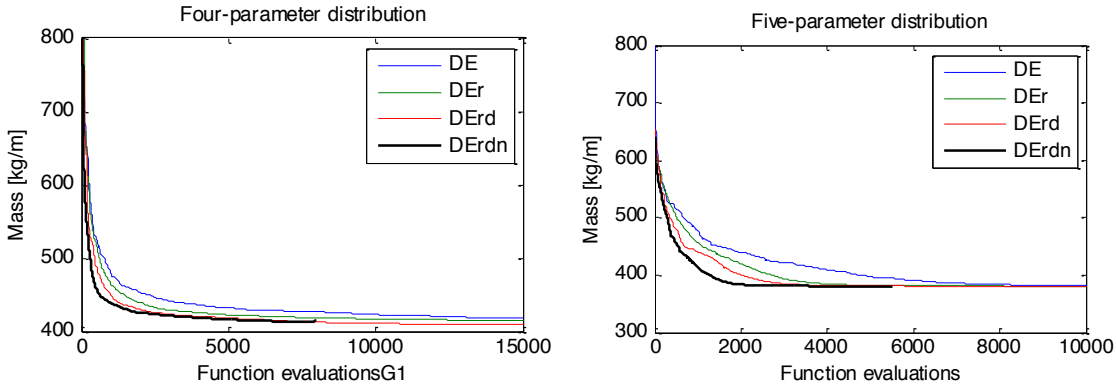


Figure 2. Comparison on the convergence of the beam's weight by different algorithms

With the same boundary condition, the five-parameter distribution can provide smaller optimal weight than that obtained by the four-parameter distribution.

Table 8. Optimisation results of Problem 1 with different support conditions

| | PP | CC | CP | CF |
|---|---|---|---|---|
| $a$ | 0.9996 | 0.9993 | 0.9999 | 0.9993 |
| $b$ | 1.0001 | 1.0001 | 1.0000 | 1.0002 |
| $c$ | 2.4692 | 2.4868 | 2.4532 | 2.5729 |
| $p$ | 4.7027 | 4.7532 | 4.6716 | 3.1583 |
| $h$ [m] | 0.1293 | 0.0568 | 0.0826 | 0.3833 |
| $W$ [kg/m] | 410.0498 | 179.8114 | 262.5041 | 1268.4540 |
| $f_1$ (Hz) | 500.0010 | 500.0015 | 500.0008 | 500.0006 |

Table 9. Optimisation results of Problem 2 with different support conditions

| | PP | CC | CP | CF |
|---|---|---|---|---|
| $a$ | 1.0000 | 1.0000 | 1.0000 | 1.0000 |
| $b$ | 1.0000 | 1.0000 | 1.0000 | 1.0000 |
| $c$ | −2.0000 | −2.0000 | 2.0000 | 2.0000 |
| $d$ | −1.5714 | −1.5711 | −1.5699 | −1.5754 |
| $p$ | 2.0439 | 2.0626 | 1.9949 | 1.4312 |
| $h$ [m] | 0.1202 | 0.0528 | 0.0769 | 0.3634 |
| $W$ [kg/m] | 381.0057 | 167.1621 | 244.0095 | 1179.7298 |
| $f_1$ (Hz) | 500.0011 | 500.0003 | 500.0009 | 500.0017 |

Furthermore, it is found that material distributions obtained for the beams with different boundary conditions are quite similar, except those corresponding to the clamped-free condition. It can be explained that the beams with support at both ends (PP, CC, CP) have a similar fundamental vibration mode, while the cantilever beam has totally different fundamental vibration behaviour. This observation is different from that of the frequency maximisation problem for FG beams conducted by Roque

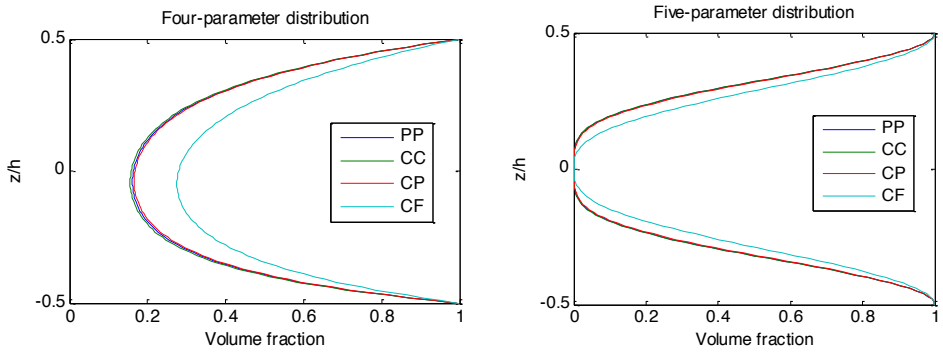


Figure 3. Optimised material distributions for different support conditions

and Martins [7], in which optimised material distributions through thickness were the same regardless boundary conditions.

The optimised volume fraction distribution along thickness is plotted for different support conditions in Fig. 3.

## 6. Conclusion

A numerical approach for weight optimisation of FG beams subjected to frequency constraints is presented. The proposed approach is a combination of the finite element method with an enhanced differential evolution algorithm. The approach is capable of accommodating different boundary conditions for FG beams. Simultaneously optimisation of the thickness and material distribution is considered. Numerical results indicate that the proposed methodology is able to solve the weight minimisation problem of FG beams under frequency constraints effectively. Moreover, the proposed DE is relatively simple and it is shown efficient for this highly non-linear optimisation problem. The superiority of the modified DE algorithm is its much less requirement for function evaluations in comparison with the conventional DE.

## Acknowledgments

This research was supported by the National University of Civil Engineering, Vietnam (NUCE) under grant number 111-2018/KHXD.

## References

[1] Miyamoto, Y., Kaysser, W. A., Rabin, B. H., Kawasaki, A., Ford, R. G. (2013). *Functionally graded materials: design, processing and applications*, volume 5. Springer Science & Business Media.

[2] Goupee, A. J., Vel, S. S. (2006). Optimization of natural frequencies of bidirectional functionally graded beams. *Structural and Multidisciplinary Optimization*, 32(6):473–484.

[3] Grandhi, R. (1993). Structural optimization with frequency constraints-a review. *AIAA Journal*, 31(12): 2296–2303.

[4] Yas, M. H., Kamarian, S., Jam, J. E., Pourasghar, A. (2011). Optimization of functionally graded beams resting on elastic foundations. *Journal of Solid Mechanics*, 3(4):365–378.

[5] Yas, M. H., Kamarian, S., Pourasghar, A. (2014). Application of imperialist competitive algorithm and neural networks to optimise the volume fraction of three-parameter functionally graded beams. *Journal of Experimental & Theoretical Artificial Intelligence*, 26(1):1–12.

[6] Kamarian, S., Yas, M. H., Pourasghar, A., Daghagh, M. (2014). Application of firefly algorithm and ANFIS for optimisation of functionally graded beams. *Journal of Experimental & Theoretical Artificial Intelligence*, 26(2):197–209.

[7] Roque, C. M. C., Martins, P. A. L. S. (2015). Differential evolution for optimization of functionally graded beams. *Composite Structures*, 133:1191–1197.

[8] Roque, C. M. C., Martins, P. A. L. S., Ferreira, A. J. M., Jorge, R. M. N. (2016). Differential evolution for free vibration optimization of functionally graded nano beams. *Composite Structures*, 156:29–34.

[9] Alshabatat, N. T., Naghshineh, K. (2014). Optimization of natural frequencies and sound power of beams using functionally graded material. *Advances in Acoustics and Vibration*, 2014.

[10] Tsiatas, G. C., Charalampakis, A. E. (2017). Optimizing the natural frequencies of axially functionally graded beams and arches. *Composite Structures*, 160:256–266.

[11] Aydogdu, M., Taskin, V. (2007). Free vibration analysis of functionally graded beams with simply supported edges. *Materials & design*, 28(5):1651–1656.

[12] Şimşek, M. (2010). Fundamental frequency analysis of functionally graded beams by using different higher-order beam theories. *Nuclear Engineering and Design*, 240(4):697–705.
[13] Thai, H.-T., Vo, T. P. (2012). Bending and free vibration of functionally graded beams using various higher-order shear deformation beam theories. *International Journal of Mechanical Sciences*, 62(1):57–66.
[14] Li, X.-F. (2008). A unified approach for analyzing static and dynamic behaviors of functionally graded Timoshenko and Euler–Bernoulli beams. *Journal of Sound and Vibration*, 318(4-5):1210–1229.
[15] Hadji, L., Khelifa, Z., Daouadji, T. H., Bedia, E. A. (2015). Static bending and free vibration of FGM beam using an exponential shear deformation theory. *Coupled Systems Mechanics*, 4(1):99–114.
[16] Chakraborty, A., Gopalakrishnan, S., Reddy, J. N. (2003). A new beam finite element for the analysis of functionally graded materials. *International Journal of Mechanical Sciences*, 45(3):519–539.
[17] Bao, G., Wang, L. (1995). Multiple cracking in functionally graded ceramic/metal coatings. *International Journal of Solids and Structures*, 32(19):2853–2871.
[18] Chi, S.-H., Chung, Y.-L. (2006). Mechanical behavior of functionally graded material plates under transverse load–Part I: Analysis. *International Journal of Solids and Structures*, 43(13):3657–3674.
[19] Ait Atmane, H., Tounsi, A., Meftah, S. A., Belhadj, H. A. (2011). Free vibration behavior of exponential functionally graded beams with varying cross-section. *Journal of Vibration and Control*, 17(2):311–318.
[20] Viola, E., Tornabene, F. (2009). Free vibrations of three parameter functionally graded parabolic panels of revolution. *Mechanics Research Communications*, 36(5):587–594.
[21] Storn, R., Price, K. (1997). Differential evolution–a simple and efficient heuristic for global optimization over continuous spaces. *Journal of Global Optimization*, 11(4):341–359.
[22] Rahnamayan, S., Tizhoosh, H. R., Salama, M. M. A. (2008). Opposition-based differential evolution. *IEEE Transactions on Evolutionary computation*, 12(1):64–79.
[23] Pholdee, N., Bureerat, S., Park, W.-W., Kim, D.-K., Im, Y.-T., Kwon, H.-C., Chun, M.-S. (2015). Optimization of flatness of strip during coiling process based on evolutionary algorithms. *International Journal of Precision Engineering and Manufacturing*, 16(7):1493–1499.
[24] Pham, H. A. (2014). Reduction of function evaluation in differential evolution using nearest neighbor comparison. *Vietnam Journal of Computer Science*, 2(2):121–131.
[25] Deb, K. (2000). An efficient constraint handling method for genetic algorithms. *Computer Methods in Applied Mechanics and Engineering*, 186(2-4):311–338.

## Appendix A

$$\alpha = \frac{B_{11}A_{55}}{(A_{11}D_{11} - B_{11}^2)}, \quad \beta = \frac{A_{11}A_{55}}{(A_{11}D_{11} - B_{11}^2)}, \quad \psi = \frac{1}{12 + \beta L^2}$$

The elements of the shape functions for axial degrees of freedom are:

$$\aleph_{u,1} = 1 - \frac{x}{L},\ \aleph_{u,2} = \frac{6x\,(x-L)\,\alpha}{L}\psi,\ \aleph_{u,3} = 3x\,(x-L)\,\alpha\psi,$$
$$\aleph_{u,4} = \frac{x}{L},\ \aleph_{u,5} = \frac{6\,(L-x)\,x\alpha}{L}\psi,\ \aleph_{u,6} = 3x\,(x-L)\,\alpha\psi$$

The elements of the shape functions for transverse degrees of freedom are:

$$\aleph_{w,1} = 0,\ \aleph_{w,2} = \frac{(L-x)\left(12 + L^2\beta + Lx\beta - 2x^2\beta\right)}{L}\psi,\ \aleph_{w,3} = \frac{(L-x)\,x\left(6 + L^2\beta - Lx\beta\right)}{L}\psi,$$
$$\aleph_{w,4} = 0,\ \aleph_{w,5} = \frac{x\left(12 + 3Lx\beta - 2x^2\beta\right)}{L}\psi,\ \aleph_{w,6} = -\frac{(L-x)\,x\,(6 + Lx\beta)}{L}\psi$$

The elements of the shape functions for rotational degrees of freedom are:

$$\aleph_{\phi,1} = 0,\ \aleph_{\phi,2} = \frac{6x\left(-L+x\right)\beta}{L}\psi,\ \aleph_{\phi,3} = \frac{\left(L-x\right)\left(12+L^2\beta-3Lx\beta\right)}{L}\psi,$$
$$\aleph_{\phi,4} = 0,\ \aleph_{\phi,5} = \frac{6\left(L-x\right)x\beta}{L}\psi,\ \aleph_{\phi,6} = \frac{x\left(12-2L^2\beta+3Lx\beta\right)}{L}\psi$$

## Appendix B

The coefficients $K_{ij}$ of the element stiffness matrix in Eq. (16) are given as follows:

$$K_{11} = -K_{14} = \frac{A_{11}}{L},\quad K_{12} = K_{15} = 0,\quad K_{13} = -K_{16} = \frac{-B_{11}}{L}$$
$$K_{22} = -K_{25} = \frac{12A_{55}}{12L+L^3\beta},\quad K_{23} = K_{26} = \frac{6A_{55}}{12+L^2\beta},\quad K_{24} = 0$$
$$K_{33} = \frac{D_{11}}{L} + \frac{3A_{55}L}{12+L^2\beta},\quad K_{34} = K_{16},\quad K_{35} = -K_{23},\quad K_{36} = -\frac{D_{11}}{L} + \frac{3A_{55}L}{12+L^2\beta}$$
$$K_{44} = K_{11},\quad K_{45} = 0,\quad K_{46} = K_{13}$$
$$K_{55} = K_{22},\quad K_{56} = -K_{23},\quad K_{66} = K_{33}$$